

Supporting information

Mechanically robust double-crosslink network functionalized graphene/polyaniline stiff hydrogels for superior performance supercapacitors

Yubo Zou^a, Rui Liu^a, Wenbin Zhong^{a,*}, Wantai Yang^b

^a College of Materials Science and Engineering, Hunan University, Changsha, 410082, P. R. China.

^b Department of Polymer Science, Beijing University of Chemical Technology, Beijing, 100029, P. R. China.

*Corresponding Author: wbzhong@hnu.edu.cn

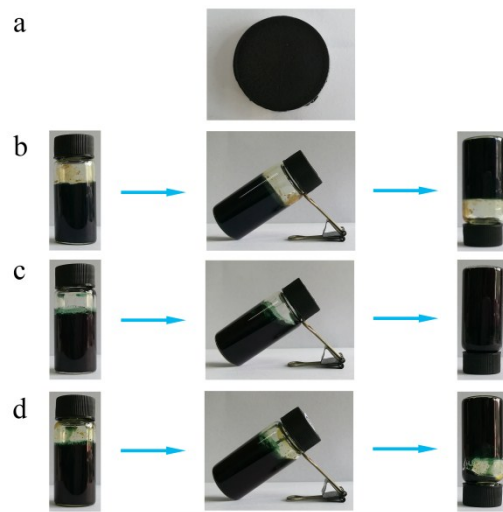


Fig. S1. The photographs of (a) functionalized graphene hydrogel (PGH) and (b-d) PANI synthesized at different conditions ((b). in PA aqueous solution, (c). in 1 M H_2SO_4 aqueous solution, (d). in the deionized water).

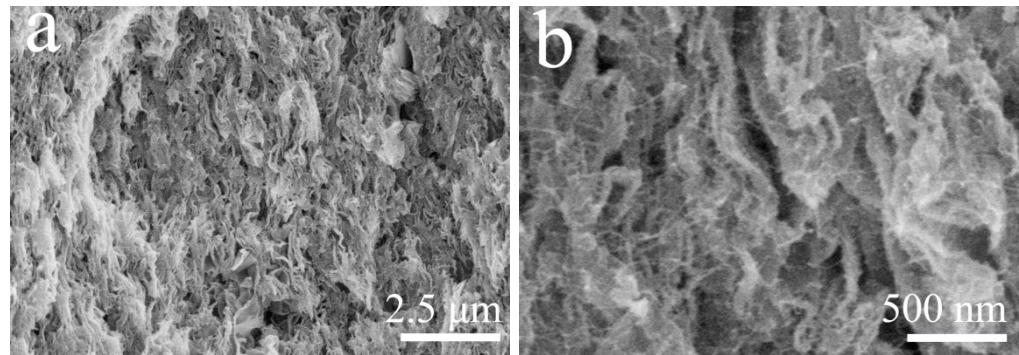


Fig. S2. The SEM images of the cross-sectional for DN-PGH/PANI_{PA} hydrogel piece tensile samples.

Table S1 The data of FT-IR for the functional groups of DN-PGH/PANI_{PA} hydrogel.

Wavenumber (cm ⁻¹)	The functional groups
3443	N—H stretching vibration
3228	O—H stretching vibration of alcohol hydroxyl or carboxyl in PGH
2905	sp ³ C—H vibration of the alkane in PA
1843	—C=O stretching vibrations in the PGH
1566, 1490	C=C stretching vibrations of quinoid and benzenoid rings in PANI chains
1290	The C—N stretching vibration in the polarized structure
1126	N=Q=N stretching mode (with Q representing the quinoid ring)
1026	C—O stretching vibration in PGH
810	Aromatic C—H bending vibration in and out of plane for the aromatic ring

Table S2 The result of XRD test for as-prepared samples.

Samples	2-Theta (degree)	d (Å)
DN-PGH/PANI _{PA}	25.3	3.52
SN-PGH/PANI _{H₂SO₄}	25.3	3.51
SN-PGH/PANI _{No-acid}	25.4	3.50
PGH	24.9	3.57

Table S3 The data of specific surface area and pore distribution for prepared hydrogel samples.

Samples	Specific surface area (m ² g ⁻¹)	Average pore diameter (nm)	Pore volume (cc g ⁻¹)
DN-PGH/PANI _{PA}	84.4	11.7	0.248
SN-PGH/PANI _{H₂SO₄}	74.4	16.3	0.304
SN-PGH/PANI _{No-acid}	108.2	10.2	0.275
PGH	18.4	6.0	0.0278

Table S4 The PANI mass loading in PGH/PANI composite hydrogels.

Sample	Mass (g)	PANI mass loading (%)
DN-PGH/PANI _{PA}	0.06977	89.0%
SN-PGH/PANI _{H₂SO₄}	0.04825	84.1%
SN-PGH/PANI _{No-acid}	0.05527	86.1%
PGH	0.00768	--

Table S5 The relative content (at.%) of N 1s species for PGH hydrogels.

Samples	Pyridinic-N	amine moieties	Pyrrolic-N	Quaternary-N
Binding energy (eV)	398.8	399.5	400.2	401.1
PGH	20.30	32.18	29.97	17.55

Table S6 The comparison of mechanical properties of the reported double-network hydrogel, mechanical enhanced conducting polymer-based and carbon-based hydrogel and/or films.

Samples	Stress	Strain	Ref.
DN-PGH/PANI_{PA} hydrogel	Tensile 1.39 MPa	0.42%	This work
PCH film, PANI-PCH film	Tensile 0.1 MPa, 0.35 MPa	290%, 300%	[S1]
	Compression 0.1 MPa	43%, 31%	
PANI@AGCAs 74.6 wt%	Compression 465 kPa	28.5%	[S2]
D-hydrogel-0.15	Tensile 5.9 MPa	748%	[S3]
physically-linked Agar/PAAc-Fe ³⁺ DN gels	Tensile 320.7 kPa	1130%	[S4]
DN-MMs hydrogels	Tensile 1.48 MPa	2100%	[S5]
P(AAm/HMA)-LP hydrogels	Tensile 1.8 MPa	2000%	[S6]
	Compression 13.5 MPa	90%	
PAAm-I-MBAm networks	Tensile 1.3 MPa	17%	[S7]
PPH hydrogel film	tensile 5.3 MPa	250%	[S8]
	compression 30 MPa	98%	
PVA-PAAm hybrid gel	Tensile 2.5 MPa	290%	[S9]
Agar/PAAm DN hydrogels	Tensile 1.0 MPa	2000%	[S10]
	Compression 38 MPa	98%	
PEDOT-PSS TN hydrogel	Tensile 0.041 MPa	89%	[S11]
PEDOT:PSS-PAAm organogels	Tensile 30 kPa	525%	[S12]
CNT bundle bucky paper	Tensile 17.1 MPa, 25.4 MPa	1.25%, 1.65%	[S13]
LEPC/PANI aerogels	Compression 1.4 MPa	20%	[S14]
PNAGA hydrogels	Tensile 1.1 MPa	1400%	[S15]
PTAA (HEDN 1) hydrogel	Compression 190 kPa	23%	[S16]
Al ₂ O ₃ nanocomposite hydrogels	Tensile 0.33 MPa	2280%	[S17]
HAPAM/PVA-6 gel	Tensile 94 kPa	1875%	[S18]
Polyaniline/poly(vinyl alcohol) cryogel	Tensile 12.2 kPa, 103 kPa	133%, 53.4%	[S19]

Polyaniline-poly(vinyl alcohol) hydrogel	Tensile 16.3 MPa	407%	[S20]
F-hydrogels	Tensile 2.1 MPa	830%	[S21]
Polyaniline-poly(vinyl alcohol) hydrogels	Tensile 16.3 MPa	407%	[S20]
GABN hydrogels	Compression 800 kPa	90%	[S22]
RGO films	Tensile 1.91 MPa	12%	[S23]
g-rGO films	Tensile 614 MPa	6%	[S24]
Graphene paper	Tensile 293.3 MPa	0.8%	[S25]
Oriented graphene hydrogel	Tensile 1.1 MPa	1.5%	[S26]

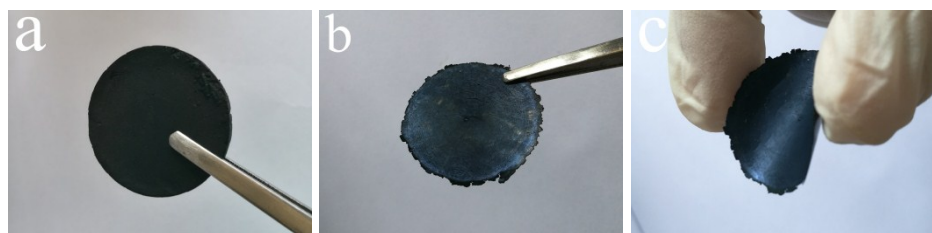


Fig. S3. The photographs of DN-PGH/PANI_{PA} hydrogels in various states. (a) Without pressuring, (b) Under pressure in its initial state, and (c) Under pressure in its bending state.

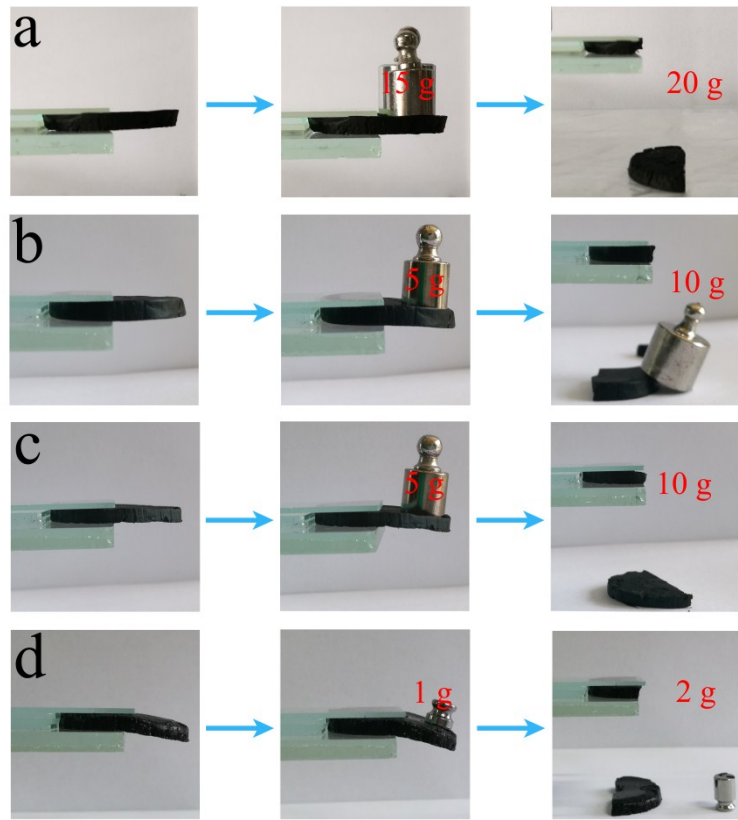


Fig. S4. The photographs of (a) DN-PGH/PANI_{PA}, (b) SN-PGH/PANI_{H₂SO₄}, (c) SN-PGH/PANI_{No-}acid and (d) PGH with a weight loading showing the stiffness. The distance between the center of weight and the center of hydrogel is calculated as ~8 mm.

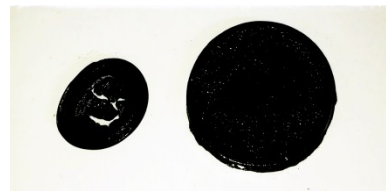


Fig. S5. The photographs of GH/PANI_{PA} (left) and DN-PGH/PANI_{PA} (right).

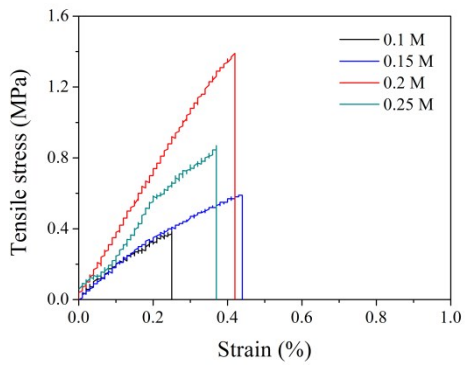


Fig. S6. The tensile stress-strain curves of double-crosslink network hydrogels with different aniline concentration (0.1 M, 0.15 M, 0.2 M (DN-PGH/PANI_{PA}), and 0.25 M).

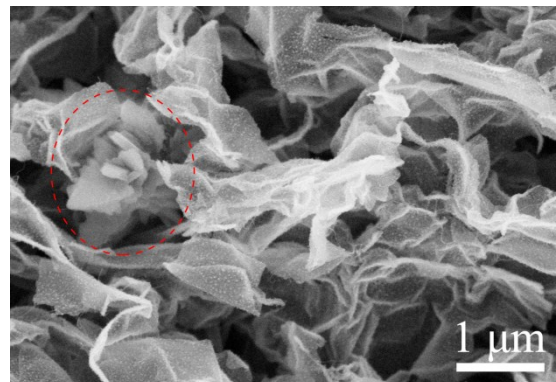


Fig. S7. The SEM image of double-crosslink network hydrogel with the aniline concentration of 0.25 M.

It can be clearly observed that the PANI bulk is aggregated in the sheets structure, which may decrease the mechanical strength of sample.

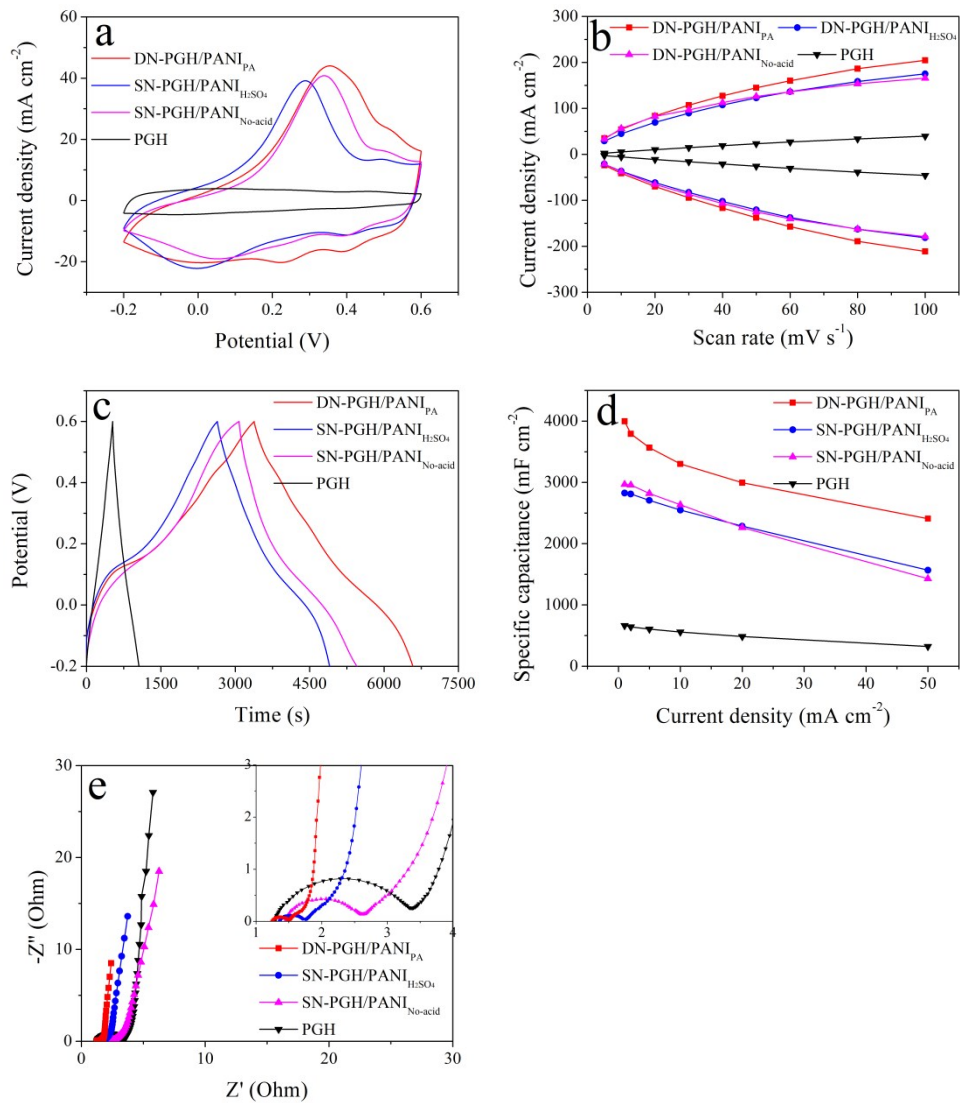


Fig. S8. The electrochemical performance of DN-PGH/PANI_{PA}, SN-PGH/PANI_{H₂SO₄}, SN-PGH/PANI_{No-acid} and PGH hydrogels based on a three-electrode system: (a) CV curves at the scan rate of 5 mV s^{-1} ; (b) The plots of the current density versus scan rate from CV curves; (c) galvanostatic charge/discharge curves at a current density of 1 mA cm^{-2} ; (d) The areal specific capacitance versus different current densities (1–50 mA cm^{-2}); (e) Nyquist plots (Inset shows the magnified high-frequency regions).

Table S7 The comparison on areal specific capacitance, volumetric specific capacitance, areal energy density and power density for carbon based PANI, PANI and carbon hydrogel and/or films supercapacitor electrodes.

Sample	C _a (mF cm ⁻²)	C _v (F cm ⁻³)	E _a (μWh cm ⁻²)	P _a (μW cm ⁻²)	Ref.
DN-PGH/PANI_{PA} hydrogel	3488.3^a	872^a	155, 67.5	200, 20015	This work
PANI(0.5 mol L ⁻¹)-PCH film	488 ^a	--	42, 30	160, 1600	[S1]
PAn@MGTF@GPs film	538 ^b	--	--	--	[S27]
CNT/PANI hydrogel film	680 ^b , 184.6 ^a	--	--	--	[S28]
PANI/GN/BC film	1320 ^a	--	120, 18	100, 4450	[S29]
SWCNT/PANI nanoribbon paper	330 ^b	40.5 ^b	--	--	[S30]
3D-RGO/PANI film	500 ^a	--	--	--	[S31]
3D-G/PANI film	1470 ^a	990 ^b , 866 ^a	64, 55	500, 15000	[S32]
CNT@PANI film	1147.12 ^a	--	50.98, 31.56	2294, 28404	[S33]
PANI/CNT composite papers	1506 ^a	--	29.4, 13.5	391, 5068	[S34]
3D rGN/PANI film	--	581 ^b	--	--	[S35]
PANI/MWCNT/PDMS film	481 ^b , 150 ^a	--	--	--	[S36]
Flexible CNF/CCS/PANI _{2:2:1} film	1838.5 ^b	--	--	--	[S37]
FGS-SSG/PANI film	1360 ^b	--	--	--	[S38]
rGO/PANI hybrid film	1600 ^b	--	--	--	[S39]
PANI/carbon cloth	787.4 ^b	--	--	--	[S40]
PANI-polyvinyl alcohol hydrogel	2320 ^b , 306 ^a	--	27.2, 23.5	200, 2600	[S8]
ABA/PANI hydrogel (HCH)	2702 ^b	--	--	--	[S41]
PANI orderly nanotube array film	237.5 ^a	--	--	--	[S42]
PANI hydrogel	522 ^a	17.4 ^c	185		[S43]
RGO hydrogel film	71 ^a	--	8.4, 4.9	4900, 40000	[S23]
3D graphene gel film	33.8 ^a	--	4.66/2.73	124000/369800	[S44]
Carbon cloth (CC)	88 ^b , 76 ^a	--	4.9	5000	[S45]

^a two-electrode cell, ^b three-electrode cell, and ^c total supercapacitor based on two-electrode cell.

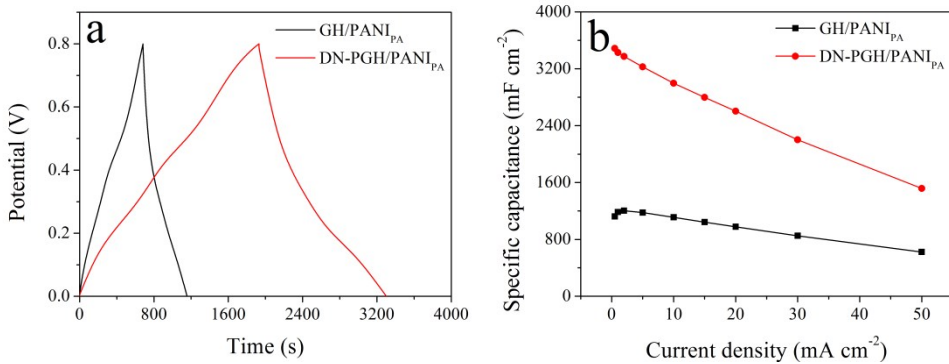


Fig. S9. (a) The galvanostatic charge/discharge curves at a current density of 1 mA cm^{-2} ; (b) the areal specific capacitance versus different current densities ($0.5\text{--}50 \text{ mA cm}^{-2}$) for GH/PANI_{PA} and DN-PGH/PANI_{PA} hydrogel.

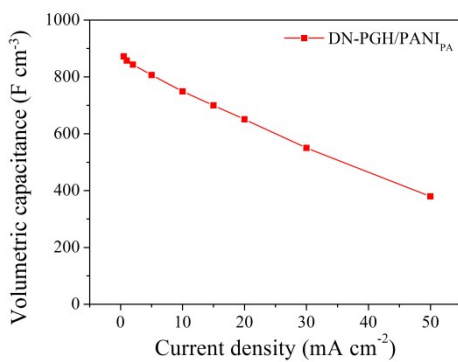


Fig. S10. The volumetric specific capacitance versus different current densities of DN-PGH/PANI_{PA} hydrogel.

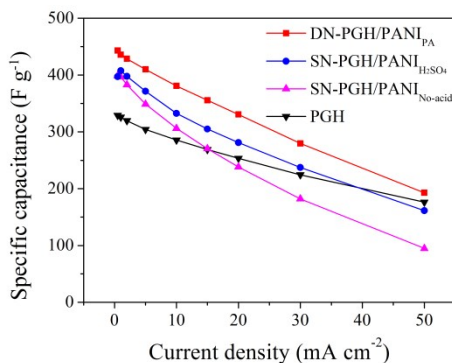


Fig. S11. The gravimetric specific capacitance of DN-PGH/PANI_{PA}, SN-PGH/PANI_{H₂SO₄}, SN-PGH/PANI_{No-acid} and PGH hydrogels.

Table S8 The comparison of gravimetric specific capacitance, volumetric specific capacitance and maximum galvanostatic energy density for carbon based PANI hydrogel and/or film electrodes based on two-electrode system.

Sample	C_g (F g ⁻¹) / I (A g ⁻¹)	C_v (F cm ⁻³)	E_g (Wh kg ⁻¹)	Ref.
DN-PGH/PANI_{PA} hydrogel	443.2 / 0.5 (mA cm⁻²)	872	9.8	This work
3D-RGO/PANI film	385 / 0.5	--	--	[S31]
G-PNF ₃₀ film	210 / 0.3	160	18.7	[S46]
PANI-rGO/CF paper	464 / 0.5	--	--	[S47]
PANI/graphene composite hydrogel	546 / 0.1, 430 / 0.5	802	12.1, 9.6	[S48]
PANI-GNRs-40	340 / 0.25	--	7.56	[S49]
flexible PANI/CNT film	400 / 0.1	--	8.9	[S50]
free-standing PANi/graphene hydrogel	223.8 / 0.4	225.42	--	[S51]
Compact PANI-CCG film	450 / 5	572	--	[S52]
Nano graphene platelet/PANI film	269 / 20 mV s ⁻¹	--	9.3	[S53]
Phase-separated 3D-PANI/CCG	712 / 1.08	--	--	[S54]
graphene wrapped PANI NFs film	844 / 1	358.3	29.3	[S55]
3D-G/PANI composite film	680	866	15.1	[S32]
HNHG-PANI ₃₀₀	526 / 0.5	763	--	[S56]

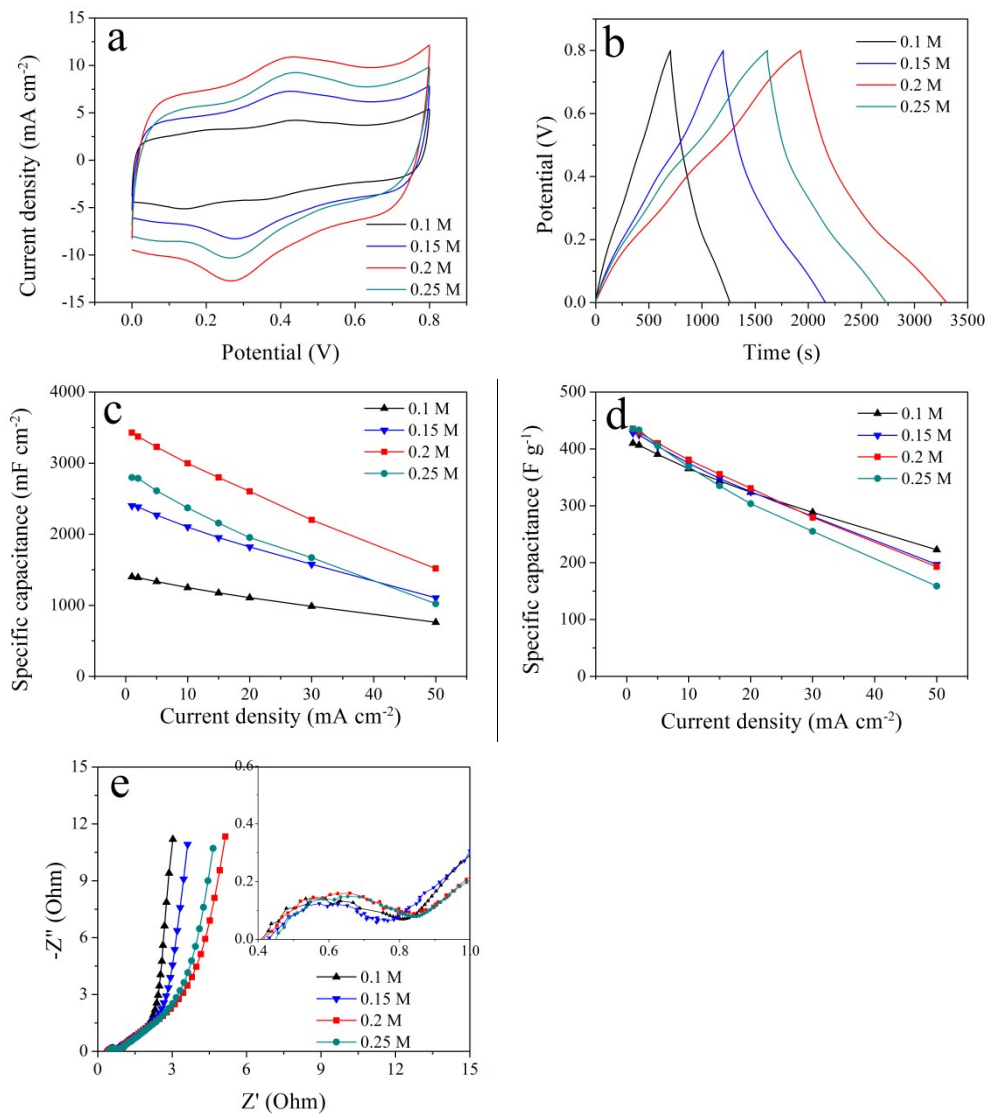


Fig. S12. The electrochemical performance of DN-PGH/PANI_{PA} hydrogels with different concentrations of aniline (0.1 M, 0.15 M, 0.2 M (DN-PGH/PANI_{PA}), and 0.25 M): (a) The CV curves at the scan rate of 5 mV s⁻¹; (b) The galvanostatic charge/discharge curves versus a current density of 1 mA cm⁻²; (c) The areal specific capacitance versus different current densities (0.5–50 mA cm⁻²); (d) Nyquist plots (Inset showed the magnified high-frequency regions); (e) The gravimetric specific capacitance versus different current densities (0.5–50 mA cm⁻²).

Table S9 The conductivity of as-prepared DN-PGH/PANI_{PA}, SN-PGH/PANI_{H₂SO₄} and SN-PGH/PANI_{No-acid}.

Samples	DN-PGH/PANI _{PA}	SN-PGH/PANI _{H₂SO₄}	SN-PGH/PANI _{No-acid}
Conductivity (S cm ⁻¹)	0.114	0.105	0.030

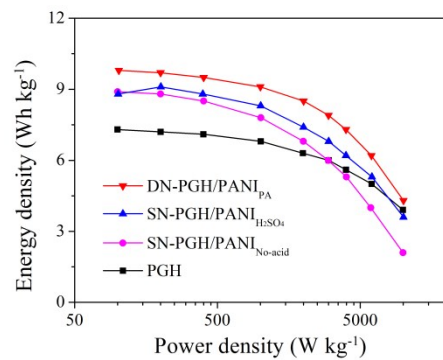


Fig. S13. Ragone plots of gravimetric energy density and power density of DN-PGH/PANI_{PA}, SN-PGH/PANI_{H₂SO₄}, SN-PGH/PANI_{No-acid} and PGH supercapacitor.

References

- [S1] K. Wang, X. Zhang, C. Li, X. Sun, Q. Meng, Y. Ma and Z. Wei. *Adv. Mater.*, **2015**, *27*, 7451-7457.
- [S2] C. H. J. Kim, D. Zhao, G. Lee and J. Liu. *Adv. Funct. Mater.*, **2016**, *26*, 4976-4983.
- [S3] P. Lin, S. Ma, X. Wang and F. Zhou. *Adv. Mater.*, **2015**, *27*, 2054-2059.
- [S4] X. Li, Q. Yang, Y. Zhao, S. Long and J. Zheng. *Soft Matter*, **2017**, *13*, 911-

- [S5] J. Hou, X. Ren, S. Guan, L. Duan, G. H. Gao, Y. Kuai and H. Zhang. *Soft Matter*, **2017**, *13*, 1357-1363.
- [S6] X. Ren, C. Huang, L. Duan, B. Liu, L. Bu, S. Guan, J. Hou, H. Zhang and G. Gao. *Soft Matter*, **2017**, *13*, 3352-3358.
- [S7] N. Rauner, M. Meuris, M. Zoric and J. C. Tiller. *Nature*, **2017**, *543*, 407-410.
- [S8] W. Li, F. Gao, X. Wang, N. Zhang and M. Ma. *Angew. Chem. Int. Ed.*, **2016**, *55*, 9196-9201.
- [S9] J. Li, Z. Suo and J. J. Vlassak. *J. Mater. Chem. B*, **2014**, *2*, 6708-6713.
- [S10] Q. Chen, L. Zhu, H. Chen, H. Yan, L. Huang, J. Yang and J. Zheng. *Adv. Funct. Mater.*, **2015**, *25*, 1598-1607.
- [S11] T. Dai, X. Qing, Y. Lu and Y. Xia. *Polymer*, **2009**, *50*, 5236-5241.
- [S12] Y. Y. Lee, H. Y. Kang, S. H. Gwon, G. M. Choi, S. M. Lim, J. Y. Sun and Y. C. Joo. *Adv. Mater.*, **2016**, *28*, 1636-1643.
- [S13] J. Zhang, D. Jiang, H.-X. Peng and F. Qin. *Carbon*, **2013**, *63*, 125-132.
- [S14] H. B. Zhao, L. Yuan, Z. B. Fu, C. Y. Wang, X. Yang, J. Y. Zhu, J. Qu, H. B. Chen and D. A. Schiraldi. *ACS Appl. Mater. Interfaces*, **2016**, *8*, 9917-9924.
- [S15] X. Dai, Y. Zhang, L. Gao, T. Bai, W. Wang, Y. Cui and W. Liu. *Adv. Mater.*, **2015**, *27*, 3566-3571.
- [S16] B. Yang, F. Yao, T. Hao, W. Fang, L. Ye, Y. Zhang, Y. Wang, J. Li and C. Wang. *Adv. Healthcare Mater.*, **2016**, *5*, 474-488.
- [S17] Y. Zhai, H. Duan, X. Meng, K. Cai, Y. Liu and L. Lucia. *Macromol. Mater.*

Eng., **2015**, *300*, 1290-1299.

- [S18] Y. Zhang, M. Song, Y. Diao, B. Li, L. Shi and R. Ran. *RSC Adv.*, **2016**, *6*, 112468-112476.
- [S19] J. Stejskal, P. Bober, M. Trchová, A. Kovalcik, J. Hodan, J. Hromádková and J. Prokeš. *Macromolecules*, **2017**, *50*, 972-978.
- [S20] W. Li, H. Lu, N. Zhang and M. Ma. *ACS Appl. Mater. Interfaces*, **2017**, *9*, 20142-20149.
- [S21] Y.-J. Liu, W.-T. Cao, M.-G. Ma and P. Wan. *ACS Appl. Mater. Interfaces*, **2017**, *9*, 25559-25570.
- [S22] L. Qiu, D. Liu, Y. Wang, C. Cheng, K. Zhou, J. Ding, V. T. Truong and D. Li. *Adv. Mater.*, **2014**, *26*, 3333-3337.
- [S23] Z. Xiong, C. Liao, W. Han and X. Wang. *Adv. Mater.*, **2015**, *27*, 4469-4475.
- [S24] M. Zhang, Y. Wang, L. Huang, Z. Xu, C. Li and G. Shi. *Adv. Mater.*, **2015**, *27*, 6708-6713.
- [S25] H. Chen, M. B. Müller, K. J. Gilmore, G. G. Wallace and D. Li. *Adv. Mater.*, **2008**, *20*, 3557-3561.
- [S26] X. Yang, L. Qiu, C. Cheng, Y. Wu, Z. F. Ma and D. Li. *Angew. Chem. Int. Ed.*, **2011**, *50*, 7325-7328.
- [S27] M. A. Memon, W. Bai, J. Sun, M. Imran, S. N. Phulpoto, S. Yan, Y. Huang and J. Geng. *ACS Appl. Mater. Interfaces*, **2016**, *8*, 11711-11719.
- [S28] S. Zeng, H. Chen, F. Cai, Y. Kang, M. Chen and Q. Li. *J. Mater. Chem. A*, **2015**, *3*, 23864-23870.

- [S29] R. Liu, L. Ma, S. Huang, J. Mei, J. Xu and G. Yuan. *New J. Chem.*, **2017**, *41*, 857-864.
- [S30] D. Ge, L. Yang, L. Fan, C. Zhang, X. Xiao, Y. Gogotsi and S. Yang. *Nano Energy*, **2015**, *11*, 568-578.
- [S31] Y. Meng, K. Wang, Y. Zhang and Z. Wei. *Adv. Mater.*, **2013**, *25*, 6985-6990.
- [S32] K. Li, J. Liu, Y. Huang, F. Bu and Y. Xu. *J. Mater. Chem. A*, **2017**, *5*, 5466-5474.
- [S33] J. Yu, W. Lu, S. Pei, K. Gong, L. Wang, L. Meng, Y. Huang, J. P. Smith, K. S. Booksh, Q. Li, J.-H. Byun, Y. Oh, Y. Yan and T.-W. Chou. *ACS Nano*, **2016**, *10*, 5204-5211.
- [S34] L. Dong, G. Liang, C. Xu, D. Ren, J. Wang, Z.-Z. Pan, B. Li, F. Kang and Q.-H. Yang. *J. Mater. Chem. A*, **2017**, *5*, 19934-19942.
- [S35] S. Wang, L. Ma, M. Gan, S. Fu, W. Dai, T. Zhou, X. Sun, H. Wang and H. Wang. *J. Power Sources*, **2015**, *299*, 347-355.
- [S36] M. Yu, Y. Zhang, Y. Zeng, M. S. Balogun, K. Mai, Z. Zhang, X. Lu and Y. Tong. *Adv. Mater.*, **2014**, *26*, 4724-4729.
- [S37] Q. Liu, S. Jing, S. Wang, H. Zhuo, L. Zhong, X. Peng and R. Sun. *J. Mater. Chem. A*, **2016**, *4*, 13352-13362.
- [S38] G. Xin, Y. Wang, X. Liu, J. Zhang, Y. Wang, J. Huang and J. Zang. *Electrochimi. Acta*, **2015**, *167*, 254-261.
- [S39] L. Zhang, D. Huang, N. Hu, C. Yang, M. Li, H. Wei, Z. Yang, Y. Su and Y. Zhang. *J. Power Sources*, **2017**, *342*, 1-8.

- [S40] T. Liu, L. Finn, M. Yu, H. Wang, T. Zhai, X. Lu, Y. Tong and Y. Li. *Nano Lett.*, **2014**, *14*, 2522-2527.
- [S41] G. Zhang, Y. Chen, Y. Deng and C. Wang. *ACS Appl. Mater. Interfaces*, **2017**, *9*, 36301-36310.
- [S42] H. Li, J. Song, L. Wang, X. Feng, R. Liu, W. Zeng, Z. Huang, Y. Ma and L. Wang. *Nanoscale*, **2017**, *9*, 193-200.
- [S43] H. Heydari and M. B. Gholivand. *New J. Chem.*, **2017**, *41*, 237-244.
- [S44] U. N. Maiti, J. Lim, K. E. Lee, W. J. Lee and S. O. Kim. *Adv. Mater.*, **2014**, *26*, 615-619.
- [S45] G. Wang, H. Wang, X. Lu, Y. Ling, M. Yu, T. Zhai, Y. Tong and Y. Li. *Adv. Mater.*, **2014**, *26*, 2676-2682.
- [S46] Q. Wu, Y. Xu, Z. Yao, A. Liu and G. Shi. *ACS Nano*, **2010**, *4*, 1963-1970.
- [S47] L. Liu, Z. Niu, L. Zhang, W. Zhou, X. Chen and S. Xie. *Adv. Mater.*, **2014**, *26*, 4855-4862.
- [S48] Y. Xu, Y. Tao, X. Zheng, H. Ma, J. Luo, F. Kang and Q. H. Yang. *Adv. Mater.*, **2015**, *27*, 8082-8087.
- [S49] L. Li, A. R. Raji, H. Fei, Y. Yang, E. L. Samuel and J. M. Tour. *ACS Appl. Mater. Interfaces*, **2013**, *5*, 6622-6627.
- [S50] C. Meng, C. Liu, L. Chen, C. Hu and S. Fan. *Nano Lett.*, **2010**, *10*, 4025-4031.
- [S51] M. Moussa, Z. Zhao, M. F. El-Kady, H. Liu, A. Michelmore, N. Kawashima, P. Majewski and J. Ma. *J. Mater. Chem. A*, **2015**, *3*, 15668-15674.

- [S52] Y. Wang, X. Yang, A. G. Pandolfo, J. Ding and D. Li. *Adv. Energy Mater.*, **2016**, *6*, 1600185.
- [S53] Y. Xu, M. G. Schwab, A. J. Strudwick, I. Hennig, X. Feng, Z. Wu and K. Müllen. *Adv. Energy Mater.*, **2013**, *3*, 1035-1040.
- [S54] J. Wu, Q. Zhang, A. Zhou, Z. Huang, H. Bai and L. Li. *Adv. Mater.*, **2016**, *28*, 10211-10216.
- [S55] N. Hu, L. Zhang, C. Yang, J. Zhao, Z. Yang, H. Wei, H. Liao, Z. Feng, A. Fisher, Y. Zhang and Z. J. Xu. *Sci. Rep.*, **2016**, *6*, 19777.
- [S56] Z. Fan, Z. Cheng, J. Feng, Z. Xie, Y. Liu and Y. Wang. *J. Mater. Chem. A*, **2017**, *5*, 16689-16701.